Correspondence of anharmonic localized vibrations to N-phonon bound states

D. Bonart*
Institute for Theoretical Physics, University of Regensburg, 93040 Regensburg, Germany
(Received 18 February 1997)

A discussion of the interrelation of anharmonic localized modes and their quantum-mechanical analogs, the so-called N-phonon bound states, is presented. For small systems and moderate quantum numbers, the ''exact'' eigenvalue spectrum is obtained by direct numerical diagonalization. A variational ansatz is presented which allows one to estimate analytically the energy levels of strongly anharmonic systems, exemplified here by a single quartic oscillator and a dimer model. It is shown that expectation values and level spacings for N-phonon bound states are in close agreement with estimates derived from the classical anharmonic localized vibrations. Finally, an estimate is given for the action of anharmonic localized modes in infinite higher-dimensional systems. This estimate suggests a threshold for anharmonic localized mode existence in three-dimensional lattices. [S0163-1829(97)03325-0]

I. INTRODUCTION

For perfect anharmonic lattices, stationary localized solutions of Newton's equations of motion can exist under certain conditions,[1–3] whereas all stationary modes of the corresponding quantum-mechanical problem may be classified with respect to a wave vector and thus are delocalized. However, in the latter case nearly degenerate bands of site-site correlated phonons have been found. These so-called N-phonon bound states were first discussed by Agranovich and co-workers.[4,5] In the weak anharmonic limit, vibrational systems may be described by suitable discrete self-trapping equations. The quantum-mechanical features of such systems have been analyzed by Scott *et al.*, first for a dimer model[6] and later for infinite linear chains[7] (a related system was also studied recently by Aubry *et al.*[8]). For a given number of phonons these authors found narrow bands of bound phonons with energies separated from the continuum of uncorrelated states. This conclusion became possible only because the approach based on the discrete self-trapping equation allows for classification of the energy levels with respect to the number of phonons.

In the general case of anharmonic systems, the number of phonons is not a good quantum number. Nevertheless, it is interesting to note that a three-atom periodic chain with harmonic and quartic intersite coupling is integrable,[9] and the corresponding quantum-mechanical problem can be solved completely.[10] Unfortunately, normal modes and localized modes are identical and no bifurcation of normal modes occurs in this system.

In general, anharmonic chains are nonintegrable. In this case one can construct an effective Hamiltonian for an infinite chain with weak cubic anharmonicities which then conserves the number of particles, as suggested by Bogdan and Kosevich.[11] However, it will be shown below that this effective Hamiltonian approach is not useful in the regime of a large number of phonons; therefore it cannot serve as a link to classical dynamics.

In the strong anharmonic case one has to diagonalize the full Hamiltonian. This method has been used to determine the eigenenergies of a H_2O molecule described by phenomenological potentials,[12] and twofold-degenerate levels were found for high quantum numbers. However, a small set of basis functions was used and a quantitative comparison with classical localized modes was not performed. In the present work a similar approach is used, but it avoids these limitations. Recently a six-atom chain was also analyzed using direct numerical diagonalization,[13] independent of the present work.[14] It was shown that N-phonon bound states persist even if the full Hamiltonian is taken into account.

The aim of the present paper is to discuss the correspondence of classical localized vibrations and bound states of phonons in more detail. The paper is organized as follows: In Sec. II a single anharmonic oscillator is analyzed classically and quantum mechanically. It is demonstrated that the effective Hamiltonian approach is limited to small quantum numbers. To overcome this limitation, a variational approach is introduced which gives approximate eigenvalues. These eigenvalues are compared with the ''exact'' eigenvalues obtained from direct diagonalization and also with semiclassical eigenvalues obtained from the Bohr-Sommerfeld quantization. In Sec. III these tools are applied to the case of a dimer with strongly anharmonic on-site potentials. First the ''exact'' eigenvalue spectrum is determined by direct numerical diagonalization of the Hamiltonian matrix. Using a variational ansatz we identify eigenstates and compare their expectation values and level spacings with classical predictions; the correspondence of N-phonon bound states and anharmonic localized modes is thereby established. In Sec. IV an estimate for the action of anharmonic localized modes in infinite higher-dimensional lattices is introduced. It is shown that for weak anharmonicity a minimum number of phonons is required for the formation of bound states in three-dimensional crystals. The paper is concluded in Sec. V.

II. SINGLE OSCILLATOR

We analyze a single anharmonic oscillator with mass m, described by the Hamiltonian,

$$H=\frac{p^2}{2m}+\frac{o_2}{2}u^2+\frac{o_4}{4}u^4, \tag{2.1}$$

with the conjugate variables (u,p). Within the effective Hamiltonian approach[11] one would model Eq. (2.1) by

$$H_{\rm eff}=\epsilon_0 a^\dagger a+\Gamma a^\dagger a^\dagger a a, \tag{2.2}$$

with Bose operators $a^\dagger$ and a. Obviously, the effective Hamiltonian has energy eigenvalues which increase quadratically in the limit of large quantum numbers. As we will see below, the semiclassical approach predicts an asymptotic growth of the energy levels as $n^{4/3}$. Hence the effective Hamiltonian approach does not apply in the classical limit.

We now introduce frequency-dependent operators $b(\omega)$ and $b^\dagger(\omega)$ (which for fixed frequency ω satisfy the usual commutator relations $[b(\omega),b^\dagger(\omega)]=1$):

$$u\equiv\sqrt{\frac{\hbar}{2m\omega}}[b(\omega)+b^\dagger(\omega)],$$

$$p\equiv -i\sqrt{\frac{\hbar m\omega}{2}}[b(\omega)-b^\dagger(\omega)]. \tag{2.3}$$

Let us consider approximate states for the nth quantum level, defined by

$$|n\rangle_\phi\equiv[b^\dagger(\omega_n)]^n|0\rangle, \tag{2.4}$$

where the effective frequency ω_n for the nth level is determined from the variational principle

$$\frac{\partial}{\partial\omega}{}_\phi\langle n|H|n\rangle_\phi\Big|_{\omega=\omega_n}=0. \tag{2.5}$$

This leads to a cubic equation in ω_n, whose solution yields the following approximation for the eigenenergies:

$$\begin{aligned}E_n&=\langle n|H|n\rangle\\&=\hbar\frac{m\omega_n^2+o_2}{4m\omega_n}(2n+1)+\frac{\hbar^2 o_4}{16m^2\omega_n^2}(6n^2+6n+3).\end{aligned} \tag{2.6}$$

For example, in the case of vanishing harmonic coupling $(o_2=0)$, one readily obtains

$$\omega_n^3=\frac{3}{2}\frac{\hbar o_4}{m^2}\left[\left(n+\frac{1}{2}\right)+\frac{1}{4(n+1/2)}\right] \tag{2.7}$$

and

$$E_n=\frac{3\hbar}{4}\left(\frac{o_4\hbar}{4m^2}\right)^{1/3}\left(n+\frac{1}{2}\right)^{2/3}(6n^2+6n+3)^{1/3}. \tag{2.8}$$

In the limit of large quantum numbers Eq. (2.8) becomes

$$E_n\approx\frac{3}{4}\left(\frac{3}{2}\right)^{1/3}m^{-2/3}o_4^{1/3}\hbar^{4/3}\left(n+\frac{1}{2}\right)^{4/3}. \tag{2.9}$$

To check the validity of this variational ansatz, we compare this last result for large n with the semiclassical Bohr-Sommerfeld quantization (see Ref. 15):

$$S=\oint p\ dq=2\pi\hbar\left(n+\frac{1}{2}\right). \tag{2.10}$$

TABLE I. Comparison of the 10 lowest ''exact'' eigenenergies with results from the variational ansatz and the semiclassical approximation for a purely quartic oscillator. We took $o_2=0$, $o_4=m=\hbar=1$.

Quantum number	Exact	Variational	Semiclassical
1	0.421	0.430	0.340
2	1.508	1.527	1.474
3	2.959	2.951	2.913
4	4.621	4.593	4.562
5	6.453	6.404	6.378
6	8.429	8.358	8.335
7	10.53	10.44	10.41
8	12.74	12.62	12.60
9	15.05	14.91	14.89
10	17.45	17.29	17.27

We now solve the classical equation of motion within the well-established rotating wave approximation (RWA) by setting $u(t)=a\cos(\omega t)$ and neglecting higher harmonics; for $o_4\geq 0$, the RWA is known to yield an accurate description of the stationary modes within a few percent, and it can easily be extended to more complex situations such as higher-dimensional vibrational systems. By evaluation of Eq. (2.10) for the RWA trajectory [with $p(t)=-m\omega a\sin(\omega t)$], we obtain

$$\omega^3=\frac{3}{2}\frac{o_4\hbar}{m^2}\left(n+\frac{1}{2}\right). \tag{2.11}$$

The total energy computed by averaging over one RWA period is

$$E_{\text{Bohr-Sommerfeld}}=\frac{3}{4}\left(\frac{3}{2}\right)^{1/3}m^{-2/3}o_4^{1/3}\hbar^{4/3}\left(n+\frac{1}{2}\right)^{4/3}, \tag{2.12}$$

which is identical with Eq. (2.9).

To check the variational ansatz in the regime of small quantum numbers, we calculate the eigenvalues of the Hamiltonian by direct numerical diagonalization, using a finite set of harmonic eigenfunctions. We denote these values to be the ''exact'' eigenenergies. In the second column of Table I, the first 10 energies are given for a purely quartic oscillator $[o_2=0,o_4=m=\hbar=1]$ based on a set of 100 harmonic eigenfunctions. Tests with 140 eigenfunctions did not change these values. The results of the variational principle shown in the third column of Table I are within a few percent. The semiclassical values given in the third column are seen to work well, beginning with the third eigenvalue. Hence the variational ansatz may be used both in the small- and large-quantum-number regimes.

III. DIMER MODEL

We now analyze a dimer model, which provides the simplest vibrational system for which a bifurcation from normal modes to anharmonic localized modes exists. The Hamiltonian describes two particles with masses m, which are coupled by harmonic forces (k_2) and which interact with a substrate via anharmonic potentials (o_2,o_4):

$$H=\frac{p_1^2}{2m}+\frac{p_2^2}{2m}+\frac{k_2}{2}(u_1-u_2)^2+\frac{o_2}{2}(u_1^2+u_2^2)+\frac{o_4}{4}(u_1^4+u_2^4). \tag{3.1}$$

This Hamiltonian is suitable for the description of a light diatomic molecule adsorbed on the surface of a heavier monatomic crystal [e.g., H_2 on Si(111)]. For reasons of simplicity we neglect cubic anharmonicities. In the case of displacements u_l normal to the surface the symmetric normal mode obeys $u_1=u_2$ and the antisymmetric mode obeys $u_1=-u_2$ (note that this classification is switched for longitudinal vibrations). For this system one can easily calculate the classical stationary vibrations within the RWA $[u_l=a_l\cos(\omega t)]$. Here one finds three solutions:

$$m\omega_1^2=o_2+\frac{3}{4}o_4a_1^2, \quad \text{symmetric: } a_1=a_2, \tag{3.2}$$

$$m\omega_2^2=o_2+2k_2+\frac{3}{4}o_4a_1^2, \quad \text{antisymmetric: } a_1=-a_2, \tag{3.3}$$

$$m\omega_3^2=o_2+k_2+\frac{3}{4}o_4a_1^2+\frac{4}{3}\frac{k_2^2}{o_4a_1^2}, \quad \text{localized: } |a_1|\neq|a_2|, \tag{3.4}$$

where the amplitude of the second particle is given by

$$a_2=\frac{o_2+k_2-m\omega_i^2}{k_2}a_1+\frac{3}{4}\frac{o_4}{k_2}a_1^3 \quad i=1,3. \tag{3.5}$$

We now define a classical expectation value of an observable A for a given classical trajectory by

$$\langle A(p_1,u_1,p_2,u_2)\rangle_{\rm cl} = \lim_{T\to\infty}\frac{1}{T}\int_0^T A[p_1(t),u_1(t),p_2(t),u_2(t)]\,dt. \tag{3.6}$$

This expectation value depends on the phase space region sampled by the classical trajectory. In particular, we consider the expectation values of the energy, of u_1u_2, and of p_1p_2; these quantities are most useful for the comparison between classical trajectories and quantum-mechanical eigenstates, as will be shown below. We compute the classical expectation values for the three RWA solutions given above. For example, the energy corresponding to a RWA solution becomes

$$\langle E\rangle_{\rm cl}=\frac{1}{4}(m\omega_i^2+o_2)(a_1^2+a_2^2)+\frac{3}{32}o_4(a_1^4+a_2^4) +\frac{1}{4}k_2(a_1-a_2)^2. \tag{3.7}$$

In Fig. 1 the energy versus $\langle u_1u_2\rangle_{\rm cl}$ and $\langle p_1p_2\rangle_{\rm cl}$ is shown for the symmetric, the antisymmetric, and the localized RWA solutions. One sees that in Fig. 1 the branch of antisymmetric vibrations exhibits a bifurcation, giving rise to the branch of localized modes.

We now come to the quantum-mechanical analysis of this system. Contrary to the classical equations of motion, the quantum-mechanical problem of stationary modes is linear and hence all eigenstates are symmetric or antisymmetric. Thus no (stationary) localization of energy is possible. A quantum-mechanical analysis of a weak anharmonic dimer was presented earlier by Scott and Eilbeck.[6] In this case one introduces a slowly varying variable ψ_l:

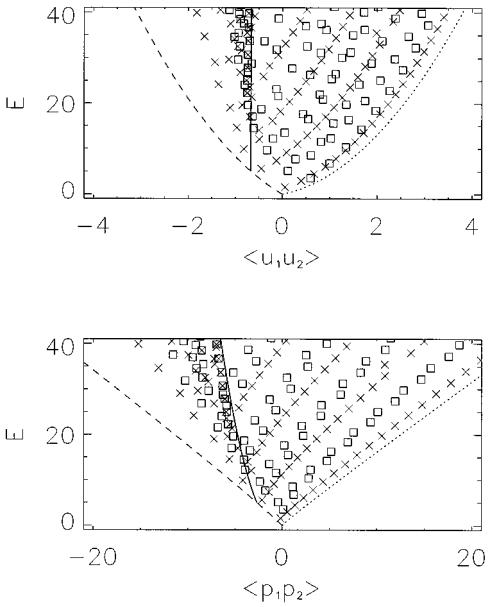

FIG. 1. Energy eigenvalues vs the expectation value of u_1u_2 (upper panel) and p_1p_2 (lower panel) for the dimer model. × and □ marks symmetric and antisymmetric eigenstates, respectively. Additionally, the corresponding classical curves for the symmetric (dotted line), antisymmetric (dashed line), and localized (solid line) RWA solutions are shown. The nearly degenerate energy levels lie close to the solid line of the localized modes. Here we used $k_2=o_2=o_4=m=\hbar=1$.

$$u_l=\psi_l\exp(-i\omega_0t)+\text{c.c.}, \tag{3.8}$$

with $m\omega_0^2=o_2$, and for $|\ddot{\psi}_l|\ll|\omega_0\dot{\psi}|$ one obtains

$$2im\omega_0\dot{\psi}_l=3o_4|\psi_l|^2\psi_l+k_2(\psi_l-\psi_{\bar{l}}), \quad \bar{l}=\begin{cases}1 & \text{for } l=2,\\ 2 & \text{for } l=1.\end{cases} \tag{3.9}$$

In this approximation not only is the energy conserved, but also

$$N=|\psi_1|^2+|\psi_2|^2, \tag{3.10}$$

and the system becomes integrable.[16] The Hamiltonian is quantized by setting $\psi=b$, $\psi^*=b^\dagger$, where $(b, b^\dagger)$ are Bose operators, and it is then diagonalized in the subspace of fixed N. This procedure corresponds to the effective Hamiltonian approach discussed above, which cannot be used for the study of the semiclassical limit because it leads to an incorrect asymptotic behavior of the energy levels.

In the strongly anharmonic case, nonparticle-conserving contributions of the Hamiltonian (3.1) become important and the corresponding classical system is nonintegrable. To obtain the eigenvalue spectrum of the Hamiltonian (3.1), a di-

rect numerical diagonalization of the Hamiltonian matrix using a finite set of harmonic eigenfunction is performed. The states are written in the form

$$|\psi\rangle=\sum_{n_1,n_2} c_{n_1 n_2}|n_1,n_2\rangle, \tag{3.11}$$

where n_1 and n_2 are the quantum numbers of the first and second oscillators. Here we use $k_2=o_2=o_4=m=\hbar=1$ and include harmonic product states $|n_1,n_2\rangle$ with $n_1+n_2 \leqslant N_{\max}$ for $N_{\max}=60$. Separate calculations of the symmetric and antisymmetric states allow a considerable reduction of the numerical effort. By lowering $N_{\max}$, the range of convergence was determined. Thus we obtain the ''exact'' eigenvalue spectrum shown in Fig. 1.

To further classify the eigenstate $|\psi\rangle$ we use the quantum-mechanical expectation values of u_1u_2, given by

$$\langle u_1u_2\rangle_{\rm qm}=\langle\psi|u_1u_2|\psi\rangle \tag{3.12}$$

and similarly for p_1p_2. In Fig. 1 the eigenenergies versus the expectation values of these correlation functions are plotted along with the corresponding classical curves (the index qm is dropped). On the branch of classical localized vibrations, pairs of nearly degenerate eigenstates are seen in Fig. 1. In the high-energy region, where the antisymmetric mode is known to be unstable, no quantum mechanical eigenstates are close to the antisymmetric branch. Since the nearly twofold-degenerate eigenstates correspond in both panels of Fig. 1 to the localized states, we conclude that they cover similar regions of phase space.

To analyze these nearly degenerate eigenstates in more detail, we now apply the variational methods introduced in the preceding section. Introducing the frequency-dependent operator $b_l(\omega)$ associated with site $l=1,2$, we consider approximate states of the form

$$|\phi\rangle\equiv|n_1,n_2\rangle_\phi=[b_1^\dagger(\omega)]^{n_1}[b_2^\dagger(\omega)]^{n_2}|0\rangle, \tag{3.13}$$

where $b_l(\omega)$ and $b_l^\dagger(\omega)$ are defined by

$$u_l\equiv\sqrt{\frac{\hbar}{2m\omega}}[b_l(\omega)+b_l^\dagger(\omega)], \tag{3.14}$$

$$p_l\equiv -i\sqrt{\frac{\hbar m\omega}{2}}[b_l(\omega)-b_l^\dagger(\omega)], \quad l=1,2. \tag{3.15}$$

The effective frequency $\omega=\omega(n_1,n_2)$ will be determined for each state $|n_1,n_2\rangle_\phi$ separately using the variational principle

$$\frac{\partial}{\partial\omega}\langle\phi|H|\phi\rangle\Big|_{\omega=\omega(n_1,n_2)}=0. \tag{3.16}$$

This real-space ansatz is constructed such that spatial variations of a state (as are present in the classical localized mode) may be described. Alternatively we first transform the Hamiltonian (3.1) to normal coordinates:

$$\tilde{u}_S=\frac{1}{\sqrt{2}}(u_1+u_2), \quad \tilde{u}_A=\frac{1}{\sqrt{2}}(u_1-u_2). \tag{3.17}$$

TABLE II. Comparison of the 12 lowest exact eigenenergies and the result of the symmetry-adapted variational ansatz $|\tilde{\phi}\rangle=|n_S,n_A\rangle_{\tilde{\phi}}$.

$E_{\rm exact}$	$E_{\tilde{\phi}}$
1.538	1.542
2.906	2.914
3.505	3.511
4.413	4.430
5.086	5.099
5.555	5.553
6.040	6.064
6.741	6.789
7.328	7.325
7.689	7.665
7.771	7.799
8.490	8.569

Then we quantize $\tilde{u}_S$ and $\tilde{u}_A$ by introducing symmetry-adapted frequency-dependent operators $\tilde{b}_i(\omega_i)$ and $\tilde{b}_i^\dagger(\omega_i)$,

$$\tilde{u}_i=\sqrt{\frac{\hbar}{2\omega_i}}[\tilde{b}_i(\omega_i)+\tilde{b}_i^\dagger(\omega_i)], \quad i=S,A, \tag{3.18}$$

and similarly for $\tilde{p}_i$. The corresponding states

$$|\tilde{\phi}\rangle=|n_S,n_A\rangle_{\tilde{\phi}}=[\tilde{b}_S^\dagger(\omega_S)]^{n_S}[\tilde{b}_A^\dagger(\omega_A)]^{n_A}|0\rangle \tag{3.19}$$

are characterized by the number of phonons in the symmetric normal mode (n_S) and the antisymmetric normal mode (n_A). Now two effective frequencies ω_S and ω_A are determined from the variational principle.

In the low-energy regime, the exact eigenenergies are close to the results obtained using the symmetry-adapted variational ansatz $|n_S,n_A\rangle_{\tilde{\phi}}$, as shown in Table II. Hence the phase space in this regime is very well described by normal coordinates. However, the near degeneracy of the eigenvalues shown in Fig. 1 is not reproduced by this variational ansatz. To identify these levels, we apply the variational ansatz in the real-space frame using Eq. (3.13). From Table III it becomes clear that the degenerate levels correspond to variational state in the real-space frame,

TABLE III. Comparison of nearly twofold-degenerate energy levels (having almost identical expectation values for u_1u_2 and p_1p_2) and the result of the variational ansatz within the real-space frame $|\phi\rangle=|n_1,n_2\rangle_\phi$.

$E_{\rm exact,1}$	$E_{\rm exact,2}$	E_ϕ	n_1	n_2
25.002	25.004	24.6	10	0
27.823	27.823	27.4	11	0
30.713	30.713	30.3	12	0
33.669	33.669	33.3	13	0
36.687	36.687	36.3	14	0
38.465	38.466	38.2	14	1
39.765	39.765	39.4	15	0
41.537	41.537	41.3	15	1

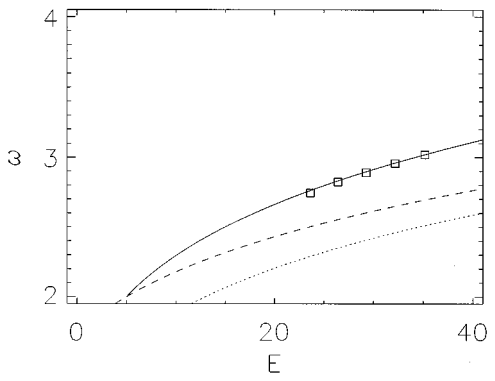

FIG. 2. Frequency of the symmetric (dotted line), antisymmetric (dashed line), and localized (solid line) classical stationary modes vs their energy. The boxes show the level spacing $(E_{N+1}-E_N)/\hbar$ between the $(N+1)$- and N-phonon bound states divided by $\hbar$ vs their center energy $(E_{N+1}+E_N)/2$, where E_N denotes the energy of the N-phonon bound state. The parameter values are the same as for Fig. 1.

$$|\psi\rangle \approx \frac{1}{\sqrt{2}}[|n,m\rangle_\phi \pm |m,n\rangle_\phi], \quad n \ll m. \tag{3.20}$$

For $n=0$ this allows for the identification of the nearly degenerate levels with the N-phonon bound states discussed earlier in literature (see, e.g., Refs. 4 and 5). Table III not only lists states of the form $|N,0\rangle$, but also lists states of the form $|N,1\rangle$, which correspond to nearly degenerate eigenstates that are close to the branch of classical localized modes in Fig. 1. To the author's knowledge, the latter form has not yet been discussed in the literature. Our numerical results suggest that for even higher energies, additional pairs of nearly degenerate states of the form $1/\sqrt{2}[|n,m\rangle_\phi \pm |m,n\rangle_\phi]$ exist for $|m-n| \gg 1$. For the interpretation of classical localized modes as a coherent superposition of nearly degenerate eigenstates, such states are necessary in order to accurately describe the motion not only of the atom with maximum amplitude but also of the atom with smaller amplitude.

Let us focus now on the states $|N,0\rangle$. As shown above they sample similar areas in phase space as the classical localized modes. To establish complete correspondence, we finally need to show that the level spacing between the N-phonon bound states fits the frequency curve of the classical localized modes (times $\hbar$). As one can see in Fig. 2, the agreement is very good. A similar comparison has also been performed by Rössler and Page[10] for the case of the integrable translationaly invariant three-atom chain in order to establish correspondence between classical and quantum-mechanical states. One can also see in Fig. 2 that the level spacing of the N-phonon bound states differs significantly from the frequencies of the normal-mode vibrations. Accordingly, the classical localized modes may be interpreted as coherent superpositions of N-phonon bound states. The results of Fig. 2 suggest that a semiclassical quantization of the localized vibration similar to the Bohr-Sommerfeld approach is feasible. In fact, setting $\oint \Sigma_l p_l \, du_l = 2\hbar(n+3/4)$ for the anharmonic localized modes, one obtains a good approximation to the energy levels of the N-phonon bound states. However, the Bohr-Sommerfeld quantization rule may be applied to integrable systems only,[15] and a justification of the factor 3/4 is missing.

IV. INFINITE HIGHER-DIMENSIONAL SYSTEMS

Strongly anharmonic higher-dimensional systems have been discussed both classically and quantum mechanically. For example the hydrogen covered Si(111) surface may give rise to an anharmonic localized mode.[17] The corresponding two-phonon bound state has been calculated by Li and Vanderbilt[18] in good agreement with the experiments of Guyot-Sionnest.[19] A similar analysis was performed by Chin *et al.*[20] for the hydrogen-covered C(111) surface. For the case of higher-dimensional ferromagnets the related two-magnon bound states have been discussed by Wortis.[21] In the limit of large quantum numbers Ivanov and Kosevich[22] have analyzed the interrelations with classical solitary waves. These authors showed that two-magnon bound states of three-dimensional magnetic systems may exist only for sufficiently strong anharmonicity.

In the small-amplitude limit the classical anharmonic localized modes are well described by the envelope solitons of the nonlinear Schrödinger equation,[23,24] which is known to have localized solutions for arbitrary small anharmonicity and arbitrary small amplitudes (in an infinite system).[25] At first sight this seems to contradict the results for magnetic systems. To investigate this problem, we consider a simple scalar model with Hamiltonian

$$H=\sum_l \frac{p_l^2}{2m}+\frac{k_2}{2}\sum_{\langle ll'\rangle}(u_l-u_{l'})^2+\frac{k_4}{4}\sum_{\langle ll'\rangle}(u_l-u_{l'})^4, \tag{4.1}$$

for the dynamics of a d-dimensional crystal. The classical localized modes may again be obtained within the RWA.

We study the classical action $\Sigma_l \oint p_l \, du_l$ of the stationary localized solution; in the harmonic limit this is proportional to the number of phonons in the mode. To calculate the action for localized modes in the strongly anharmonic limit, we use in one dimension an 80-atomic chain, in two dimensions a (200×200)-square lattice, and in three dimensions a $(20\times20\times20)$-cubic lattice. We consider the stable anharmonic localized mode, i.e., in one dimension the $(0,-1,1,0)$ mode[3] and in two and three dimensions the $(0,1,0)$ modes.[2] These modes are easily calculated using the self-consistency scheme described in Ref. 26.

To compute the action of anharmonic localized modes in the small-amplitude limit, we apply the continuum approximation of the nonlinear Schrödinger equation.[23,24] Here one sets

$$u_l(t)=(-1)^{|l|}\psi(t,r_l)e^{-i\omega t}+\text{c.c.}, \tag{4.2}$$

where the factor $(-1)^{|l|}$ means that neighboring particles move antiphase. The slowly varying spatial and temporal envelope ψ is governed by the nonlinear Schödinger equation (NLS)

$$i\partial_t\psi=\mathcal{K}_2\Delta\psi+\mathcal{K}_4|\psi|^2\psi. \tag{4.3}$$

The parameters $\mathcal{K}_2$, $\mathcal{K}_4$ may be obtained from knowledge of the harmonic dispersion and from perturbation theory.[27] Sta-

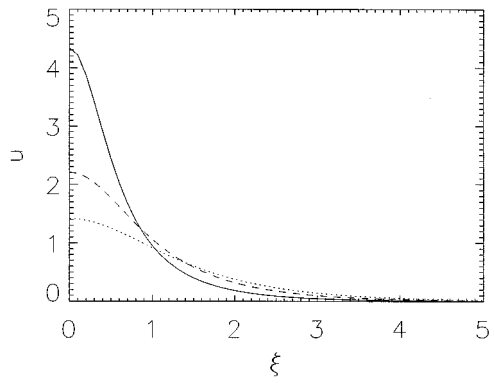

FIG. 3. Radially symmetric solution $u(\xi)$ for the nonlinear Schrödinger equation in one dimension (dotted line), two dimensions (dashed line), and three dimensions (solid line).

tionary solutions of Eq. (4.3) are well known[25] and radially symmetric localized modes may be found using the ansatz $\psi(r,t)=\psi(r)e^{-i\lambda t}$. The equations for the radially symmetric stationary problem in d dimensions are rescaled by

$$\xi=\sqrt{\lambda/\mathcal{K}_2}\,r,$$

$$u(\xi)=\sqrt{\mathcal{K}_4/\lambda}\;\psi(\xi)$$

to give

$$u(\xi)=u''+\frac{(d-1)}{\xi}u'+u^3. \tag{4.4}$$

Note that u may be chosen to be real. The solutions of Eq. (4.4) are known analytically for $d=1$. For $d=2,3$ one easily obtains accurate solutions numerically by a ''shooting and matching method'' (see, e.g., Ref. 28). The solutions are shown in Fig. 3.

We can use this rescaled function to estimate the action of an anharmonic localized mode in closed form,

$$S=\sum_l \oint p_l\,du_l=\pi\omega\sum_l a_l^2$$

$$\approx 4\pi\omega\int d^dr\,|\psi|^2,$$

$$=4\pi\omega(2\psi_0)\Omega_d M_d\left[\frac{\mathcal{K}_2}{\mathcal{K}_4}\right]^{d/2}\left[\frac{\alpha(d)}{\psi_0}\right]^{d-2},$$

where $2\psi_0$ denotes the maximum amplitude of the mode. The integrals were evaluated numerically, yielding

$$\alpha(d)=\begin{cases}\sqrt{2}, & d=1,\\ 2.21, & d=2,\\ 4.34, & d=3,\end{cases}$$

$$\omega(2\psi_0)=2dk_2+4\mathcal{K}_4\left(\frac{|\psi_0|}{\alpha(d)}\right)^2,$$

$$\Omega_d=\begin{cases}2, & d=1,\\ 2\pi, & d=2,\\ 4\pi, & d=3\end{cases}$$

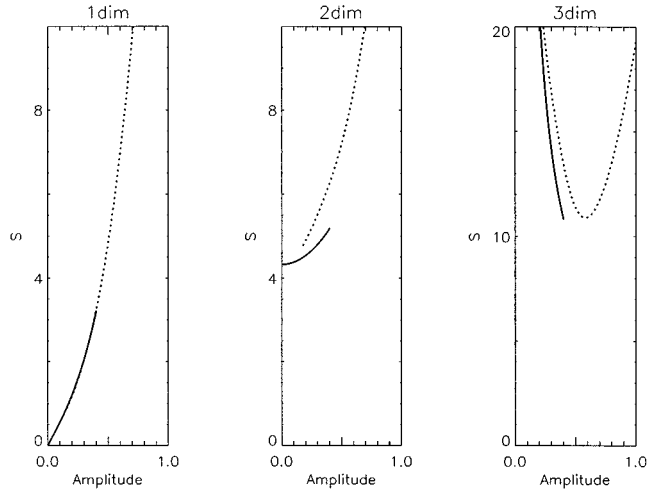

FIG. 4. Action of the localized modes for the scalar model vs the amplitude for one-, two-, and three-dimensional lattices with $k_2=k_4=1$. The dotted line corresponds to the RWA solutions of the discrete lattice and the solid line to the continuum approximation of the NLS.

$$M_d=\int_0^\infty d\xi\;\xi^{d-1}u(\xi)=\begin{cases}2.1, & d=1,\\ 1.9, & d=2,\\ 1.5, & d=3.\end{cases}$$

The resulting estimates for the action of anharmonic localized modes in one-, two-, and three-dimensional lattices are shown in Fig. 4. The most striking feature is that the action diverges in the three-dimensional lattice for small amplitudes. Hence the small-amplitude limit does *not* correspond to the limit of a few phonons. For large amplitudes the action also grows, leading to a nonzero minimum. This minimum value divided by $\hbar$ corresponds to the minimum number of phonons required for the existence of a bound state; thus the apparent discrepancy mentioned above between earlier works on two-magnon bound states and the intuitive picture based on the NLS is resolved. A similar estimate for the energy of anharmonic localized vibrations was found independently by Flach *et al.*[29]

V. CONCLUSION

In this paper we have presented an analysis of the interrelation between anharmonic localized modes and the corresponding N-phonon bound states which arise in a quantum-mechanical treatment of certain vibrational systems. The first section presents a variational ansatz which yields a good estimate for the energy levels of a single, strongly anharmonic oscillator over the entire range of quantum numbers. Then the ''exact'' eigenenergies of an anharmonic dimer model were obtained by direct numerical diagonalization and a comparison was made with the result of the variational ansatz. Nearly twofold-degenerate eigenstates were identified, which correspond to the N-phonon bound states previously discussed in the literature within an effective Hamiltonian approach.[4,5,11] Note that the classification of N-phonon bound states in these earlier investigations was possible only

because the effective Hamiltonian conserves the number of phonons. We have shown here that for Hamiltonians which do *not* conserve the number of phonons, such states still exist and approximate quantum numbers may be determined using a variational ansatz. Comparison of the level spacings and of expectation values for selected correlation functions of these nearly degenerate eigenstates with semiclassical estimates derived from the classical localized modes revealed a close correspondence. For the case of infinite higher-dimensional lattices, an estimate for the action of localized modes was given which suggests that anharmonic localized vibrations can exist in three-dimensional lattices only for a sufficiently high number of bound phonons, in agreement to earlier investigation on magnetic systems.

ACKNOWLEDGMENTS

The author would like to thank A. P. Mayer for support and stimulating discussions and J. B. Page for careful reading of the manuscript. This work was also supported by the Deutsche Forschungsgemeinschaft, Grant No. Ma 1074/54-2, NSF Grant No. DMR 9510182, and by the Feodor Lynen program of the Humboldt foundation.

*Current address: Department of Physics and Astronomy, Arizona State University, Tempe, Arizona 85287-1504.

[1] A. S. Dolgov, Fiz. Tverd. Tela (Leningrad) **28**, 1641 (1986) [Sov. Phys. Solid State **28**, 907 (1986)].
[2] A. J. Sievers and S. Takeno, Phys. Rev. Lett. **61**, 970 (1988).
[3] J. B. Page, Phys. Rev. B **41**, 7835 (1990).
[4] V. M. Agranovich, O. A. Dubovsky, and A. V. Orlov, Phys. Lett. A **119**, 83 (1986).
[5] V. M. Agranovich, O. A. Dubovsky, and A. V. Orlov, Solid State Commun. **70**, 675 (1989).
[6] A. C. Scott and J. C. Eilbeck, Phys. Lett. A **119**, 60 (1986).
[7] A. C. Scott, J. C. Eilbeck, and H. Gilhøj, Physica D **78**, 194 (1994).
[8] S. Aubry, S. Flach, K. Kladko, and E. Olbrich, Phys. Rev. Lett. **76**, 1607 (1996.
[9] F. Fischer, Ann. Phys. (Leipzig) **2**, 296 (1993).
[10] T. Rössler and J. B. Page, Phys. Rev. B **51**, 11 382 (1995).
[11] M. M. Bogdan and A. M. Kosevich, Sov. J. Low Temp. Phys. **2**, 391 (1977).
[12] R. T. Lawton and M. S. Child, Mol. Phys. **40**, 773 (1980).
[13] W. Z. Wang, J. T. Gammel, A. R. Bishop, and M. I. Salkola, Phys. Rev. Lett. **76**, 3598 (1996).
[14] D. Bonart, Ph.D. thesis, Regensburg, 1996.
[15] M. Tabor, *Chaos and Integrability in Nonlinear Dynamics* (Wiley, New York, 1989).
[16] J. C. Eilbeck, P. S. Lomdahl, and A. C. Scott, Physica D **16**, 318 (1985).
[17] U. Schröder, D. Bonart, and A. P. Mayer, Physica B **219&220**, 390 (1996).
[18] X. P. Li and D. Vanderbilt, Phys. Rev. Lett. **69**, 2543 (1992).
[19] P. Guyot-Sionnest, Phys. Rev. Lett. **67**, 2323 (1991).
[20] R. P. Chin, X. Blase, Y. R. Shen, and S. G. Louie, Europhys. Lett. **30**, 399 (1995).
[21] M. Wortis, Phys. Rev. **132**, 85 (1963).
[22] B. A. Ivanov and A. M. Kosevich, Zh. Eksp. Teor. Fiz. **72**, 2000 (1977) [Sov. Phys. JETP **45**, 1050 (1997).
[23] A. M. Kosevich and A. S. Kovalev, Zh. Eksp. Teor. Fiz. **67**, 1793 (1974) [Sov. Phys. JETP **40**, 891 (1975)].
[24] K. Yoshimura and S. Watanabe, J. Phys. Soc. Jpn. **60**, 82 (1991).
[25] J. J. Rasmussen and K. Rypdal, Phys. Scr. **33**, 481 (1986).
[26] D. Bonart, A. P. Mayer, and U. Schröder, Surf. Sci. **313**, 427 (1994).
[27] D. Bonart, A. P. Mayer, and U. Schröder, in Proceedings of Heriot-Watt University, the Conference on Nonlinear Coherent Structures in Physics and Biology, Edinburgh, July 10-14, 1995, edited by D. B. Duncan and J. C. Eilbeck, published on WWW: http://www.ma.hw.ac.uk/solitons/procs/.
[28] W. H. Press, B. P. Flannery, S. A. Teukolsy, and W. T. Vetterling, *Numerical Recipes* (Cambridge University Press, Cambridge, England, 1986).
[29] S. Flach, K. Kladko, and R. S. MacKay, Phys. Rev. Lett. **78**, 1207 (1997).